Supplementary Information

Supplementary Methods:

DNA preparation

Cell pellets were digested with proteinase K, DNA was extractedusing QIAamp DNA mini kit (Qiagen®) and DNA concentration was measured by NanoDrop (Thermoscientific®). Quality of DNA was controlled on 1% agarose gel.

Copy number variation analysis

Copy number variation (CNV) analysis was performed using the iSelect Infinium HumanOmniExpress v1.0 Illumina® chip platform. Normalized intensity signals were generated from the Illumina GenomeStudio software and then processed by tQN[1]. The normalized data was analyzed for CNV and loss of heterozygosity using GPHMM algorithm[2]. Gain was defined as copy number (CN) 1 or more over a sample ploidy and loss as CN 1 or more below a sample ploidy. High amplification was defined as CN 3 or more over a sample ploidy and homozygous deletion as CN=0 or CN 1 or 0 in a sample with tetraploid genome. Copy neutral loss-of-heterozygosity (CN-LOH) was defined as loss of heterozygosity and CN that equal the estimated sample ploidity.

Whole Exome Sequencing

Exome capture was performed using Agilent® kit Capture Agilent SureSelect All exon v5+UTR according to manufacturer protocol and for 5 samples by Nextera rapid capture exome kit. A

paired-end 2x75 bases sequencing was performed by HiSeq 2000. Data analysis used GATK best practices pipeline[3], consisted of the following steps: (i) adaptor sequence removing using Cutadapt[4,] (ii) low quality reads removing using Trimomatics[5], (iii) alignment using BWA[6]with hg19 as the reference genome, (iv) quality control using Qualimap[7], (v) deduplication using samtools[8], (vi)somatic mutation analysis using Mutect[9] for tumor samples with blood-paired DNA data, and (vii)GATK HaplotypeCaller [3] for tumor samples without blood-paired DNA data. For the tumor samples without blood-paired DNA data, only mutations that were defined as "novel" (*i.e.* not described in dbSNP) were considered.

RNA chip analysis

Cell pellets were mixed with Trizol/chloroform solution and RNA was extractedusing RNeasy Lipid Tissu mini kit (Qiagen®). RNA concentrations were measured by NanoDrop (Thermoscientific®) and quality was controlled on Agilent® 2100 bioanalyzer. Expression analysis was performed using the Human Genome U133 Plus 2.0 array and Affymetrix® 3'IVT Express Labeling kit. Data processing was performed using Bioconductor[10]. Packages Affy[11] and Simplaffy[12] were used for gathering and normalizing the raw CEL files. The normalization method was Robust Multiarray Averaging (RMA). Quality control was carried using AffyPLM package[13]. For genes represented by more than one probe, the probe with the maximal expression variability was chosen and the other probes were discarded. Limma package[14] was used for differential expression analysis ($p<0.05$, with False Discovery Rate (FDR) correction). GBM subtype[15] classification was performed using ssGSEA in GenePattern[16], as reported in Brennan *et al*[17].

RNA sequencing (RNA-Seq) analysis

Libraries were generated from total RNA and constructed according to manufacturer protocols. Paired end sequencing (2 x 150 bp) was performed by Nextseq 500 machine using High Output kit (300 cycles). The data analysis consisted of the following steps: (i) assessment of quality of raw reads with FastQC[18], (ii) trimming, including adaptors cutting and exclusion of reads below 40, with Trimmomatic[5], (iii) alignment of processed reads on human reference genome hg19 with Tophat2[19] -default options, except -g=1-, (iv) counting of the number of reads overlapping a gene with HTSeq-count[20]and, (v) normalization and differential expression analysis with DESeq2[21] ($p<0.05$ in Wald test with FDR correction).Fusion identification analysis was performed with Tophat-fusion and Tophat-fusion-post[22] (tophat-2.0.13). Candidate fusion products were filtered using the following criteria: (i) at least one of the genes is a COSMIC gene, (ii) pseudogenes were filtered out, and (iii) at least one spanning read and two spanning pairs supporting the fusion.

TP53 staining

Formalin-fixed paraffin-embedded tissue sections were processed for deparaffinization and immunolabelling by a fully automatic immunohistochemistrysystem, Ventana benchmark XT System (Roche, Basel, Switzerland), using a streptavidin-peroxidase complex with diaminobenzidine as the chromogen.The primary antibody was the monoclonal mouse anti P53 clone DO-7 (Dako, Denmark), dilution 1/100.

Visualization

Visualization was performed using R packages ggplot2[23], CopyNumber[24] and Gitools[25]

Accession codes

All whole-exome sequencing and RNAseq data have been deposited at the European Genome-phenome Archive (EGA), which is hosted by the European Bioinformatics Institute (EBI), under the accession code EGAS00001001871. Array based mRNA expression and SNP data can be accessed through ArrayExpress under accession numbers E-MTAB-4803 for mRNA expression data, and E-MTAB-4804 for SNP data.

References

1. Staaf J, Vallon-Christersson J, Lindgren D, et al. Normalization of Illumina Infinium whole-genome SNP data improves copy number estimates and allelic intensity ratios. *BMC bioinformatics.* 2008; 9:409.

2. Li A, Liu Z, Lezon-Geyda K, et al. GPHMM: an integrated hidden Markov model for identification of copy number alteration and loss of heterozygosity in complex tumor samples using whole genome SNP arrays. *Nucleic acids research.* 2011; 39(12):4928-4941.

3. DePristo MA, Banks E, Poplin R, et al. A framework for variation discovery and genotyping using next-generation DNA sequencing data. *Nature genetics.* 2011; 43(5):491-498.

4. Martin M. Cutadapt removes adapter sequences from high-throughput sequencing reads. *EMBnet.journal.* 2011; 17(1):10-12.

5. Bolger AM, Lohse M, Usadel B. Trimmomatic: a flexible trimmer for Illumina sequence data. *Bioinformatics (Oxford, England).* 2014; 30(15):2114-2120.

6. Li H, Durbin R. Fast and accurate short read alignment with Burrows-Wheeler transform. *Bioinformatics (Oxford, England).* 2009; 25(14):1754-1760.

7. García-Alcalde F, Okonechnikov K, Carbonell J, et al. Qualimap: evaluating next-generation sequencing alignment data. *Bioinformatics (Oxford, England).* 2012; 28(20):2678-2679.

8. Li H, Handsaker B, Wysoker A, et al. The Sequence Alignment/Map format and SAMtools. *Bioinformatics (Oxford, England).* 2009; 25(16):2078-2079.

9. Cibulskis K, Lawrence MS, Carter SL, et al. Sensitive detection of somatic point mutations in impure and heterogeneous cancer samples. *Nature biotechnology.* 2013; 31(3):213-219.

10. Huber, W, Carey, et al. Orchestrating high-throughput genomic analysis with Bioconductor. *Nature methods.* 2015; 12(2):115-121.

11. Gautier L, Cope L, Bolstad BM, Irizarry RA. affy—analysis of Affymetrix GeneChip data at the probe level. *Bioinformatics.* 2004; 20(3):307-315.

12. Miller CJ. *simpleaffy: Very simple high level analysis of Affymetrix data*.

13. Brettschneider J, Collin F, Bolstad BM, Speed TP. Quality Assessment for Short Oligonucleotide Microarray Data. *Technometrics.* 2008; 50(3):241-264.

14. Ritchie ME, Phipson B, Wu D, et al. limma powers differential expression analyses for RNA-sequencing and microarray studies. *Nucleic acids research.* 2015; 43(7):e47.

15. Verhaak RGW, Hoadley KA, Purdom E, et al. Integrated genomic analysis identifies clinically relevant subtypes of glioblastoma characterized by abnormalities in PDGFRA, IDH1, EGFR, and NF1. *Cancer Cell.* 2010; 17(1):98-110.

16. Reich M, Liefeld T, Gould J, Lerner J, Tamayo P, Mesirov JP. GenePattern 2.0. *Nature genetics.* 2006; 38(5):500-501.

17. Brennan CW, Verhaak RG, McKenna A, et al. The somatic genomic landscape of glioblastoma. *Cell.* 2013; 155(2):462-477.

18. FastQC. A quality control tool for high throughput sequence data. *Babraham Bioinformatics Web site* http://www.bioinformatics.babraham.ac.uk/projects/fastqc/. Accessed January, 10 2015.

19. Kim D, Pertea G, Trapnell C, Pimentel H, Kelley R, Salzberg SL. TopHat2: accurate alignment of transcriptomes in the presence of insertions, deletions and gene fusions. *Genome biology.* 2013; 14(4):R36.

20. Anders S, Pyl PT, Huber W. HTSeq--a Python framework to work with high-throughput sequencing data. *Bioinformatics.* 2015; 31(2):166-169.

21. Anders S, McCarthy DJ, Chen Y, et al. Count-based differential expression analysis of RNA sequencing data using R and Bioconductor. *Nat Protoc.* 2013; 8(9):1765-1786.

22. Kim D, Salzberg SL. TopHat-Fusion: an algorithm for discovery of novel fusion transcripts. *Genome biology.* 2011; 12(8):R72.

23. Wickham H. *ggplot2: elegant graphics for data analysis*: Springer New York; 2009.

24. Nilsen G, Liestol K, Van Loo P, et al. Copynumber: Efficient algorithms for single- and multi-track copy number segmentation. *BMC genomics.* 2012; 13:591.

25. Perez-Llamas C, Lopez-Bigas N. Gitools: analysis and visualisation of genomic data using interactive heat-maps. *PloS one.* 2011; 6(5):e19541.

Supplementary Figure 1.

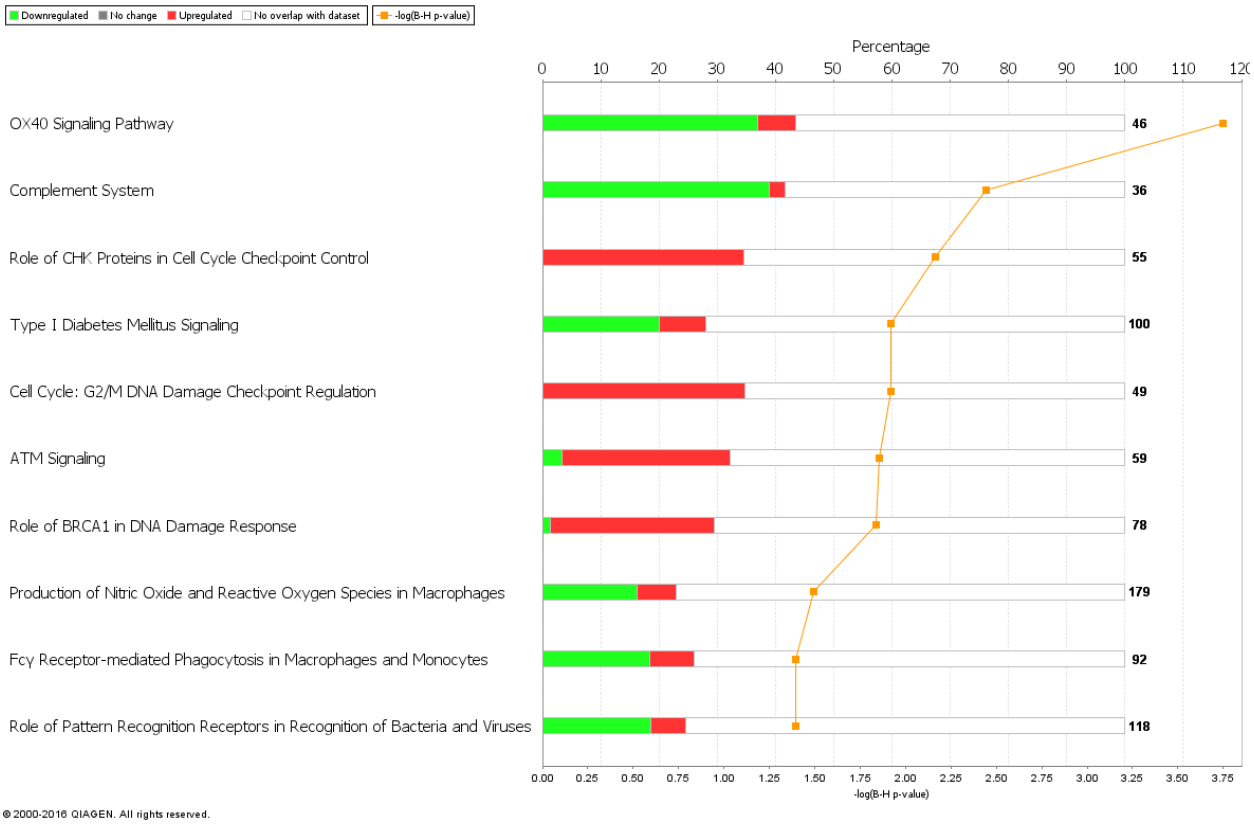

Supplementary Figure 1. Ingenuity pathway analysis for the microarray differentially expressed genes. Corresponds to the pathways described Figure 3c but showing the number of over and under expressed genes for each pathway.

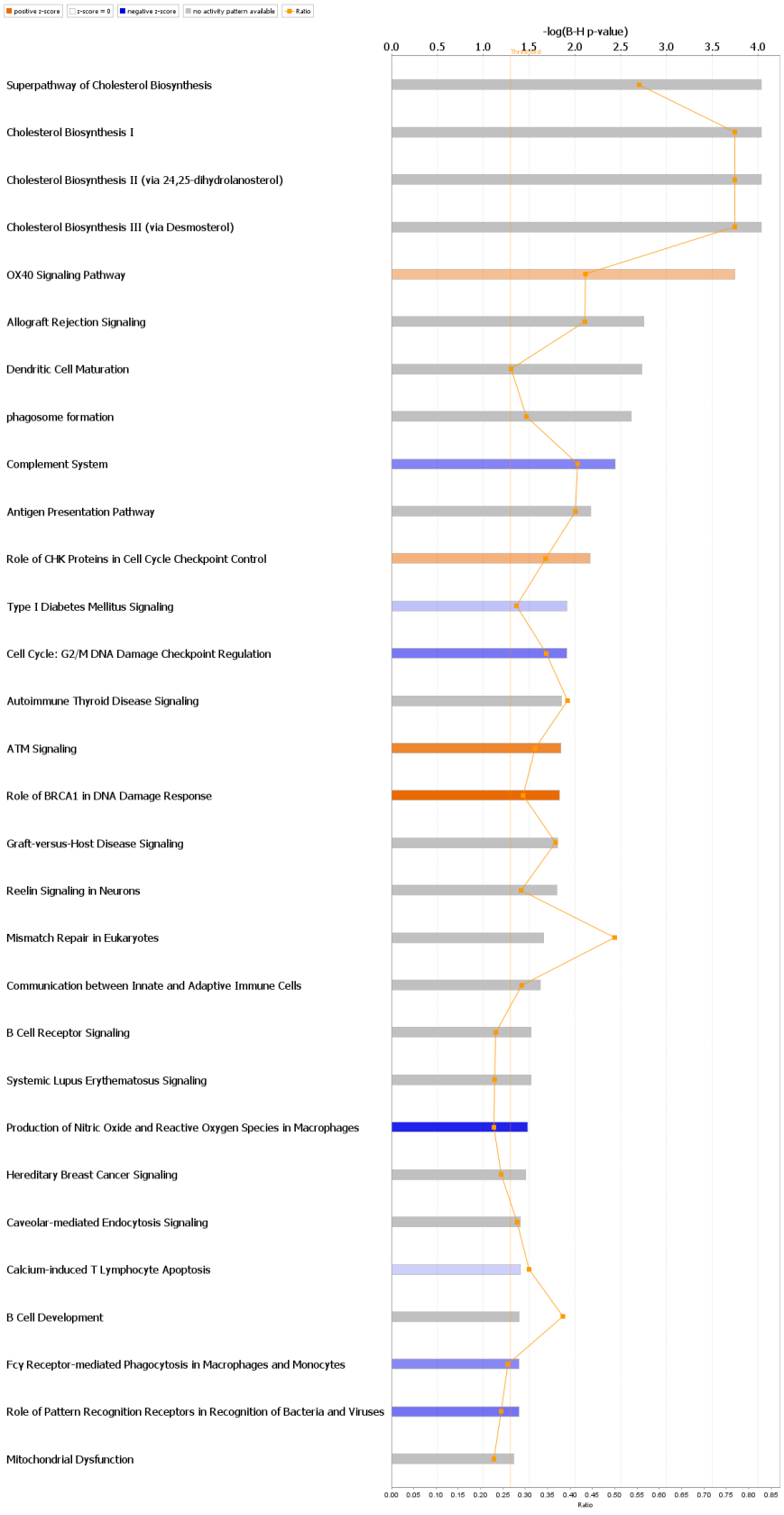

Supplementary Figure 2.

Supplementary Figure 2. Complete Ingenuity pathway analysis identified for the microarray differentially expressed genes (including pathways for which activation direction was not inferred). Orange denotes pathway activation in PDCL compared to parental tumors and blue denoted pathway inhibition, grey denotes that activation direction could not be inferred.

Supplementary Figure 3.

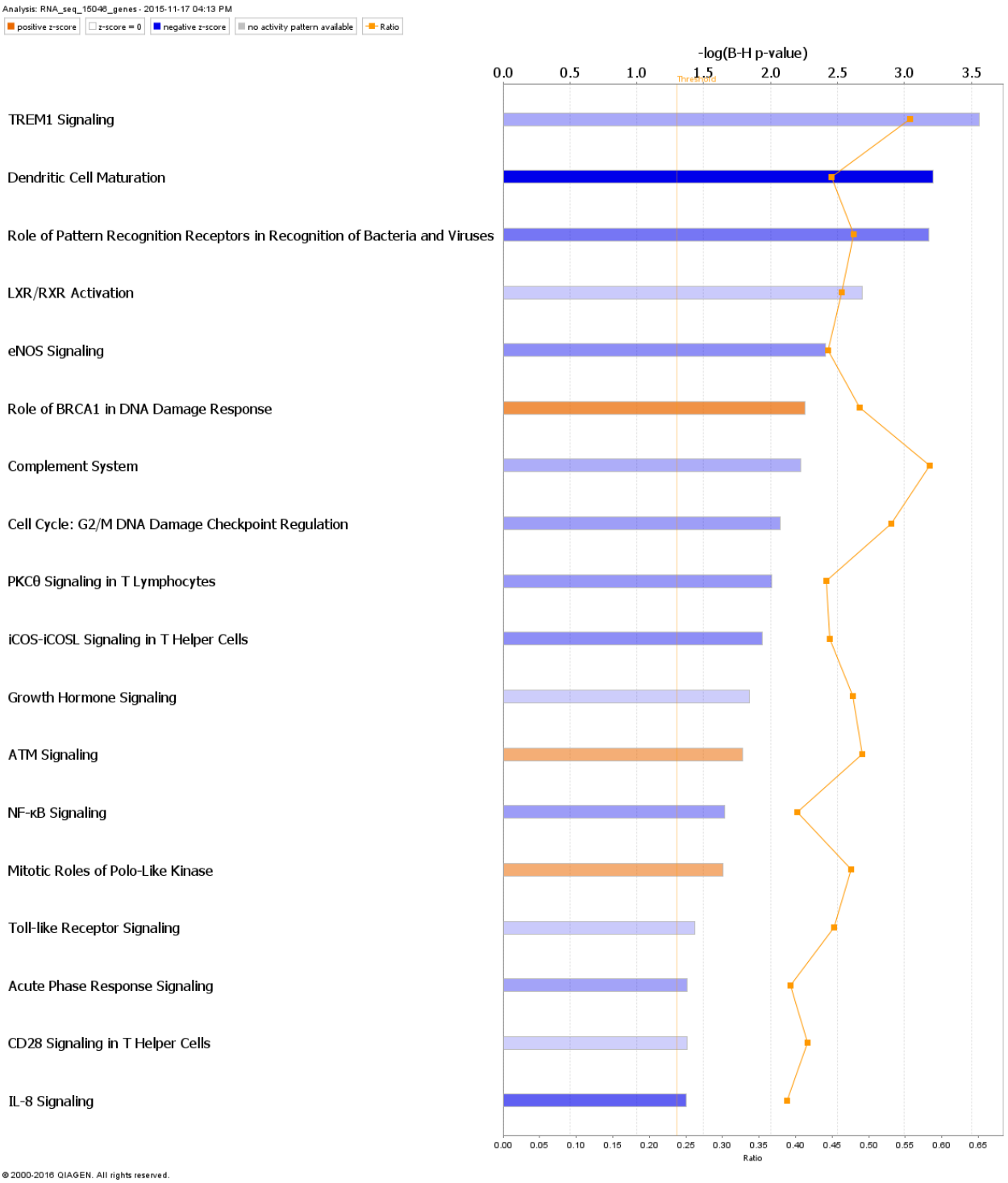

Supplementary Figure 3. Ingenuity pathway analysis for RNA seq differentially expressed genes. Only pathways for which activation direction could be inferred are shown, colored by

activation direction. Orange denotes pathway activation in PDCL compared to parental tumors and blue denoted pathway inhibition.

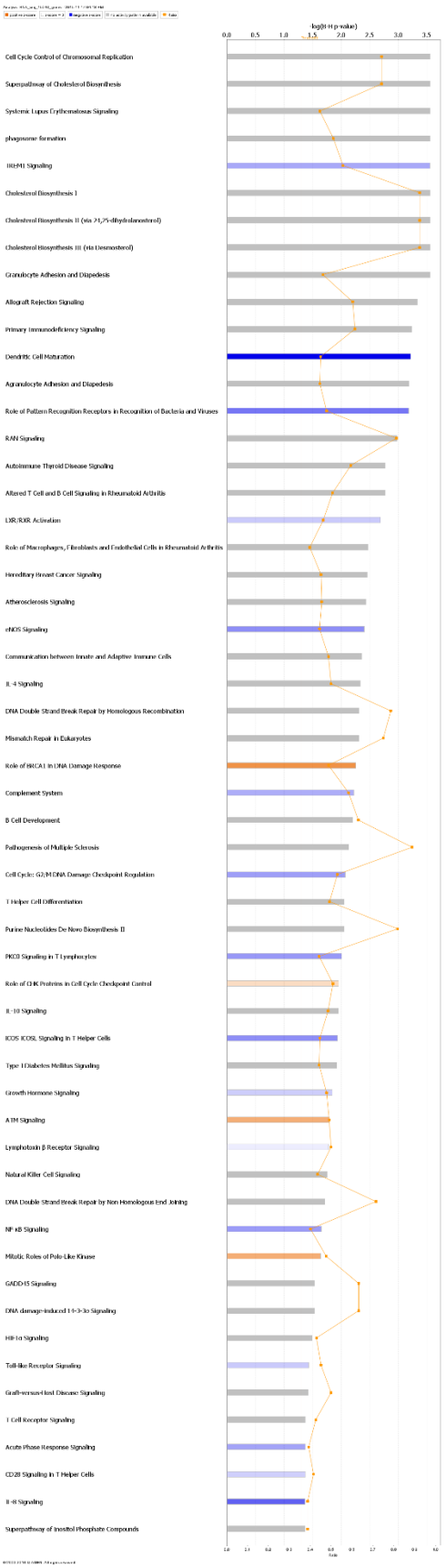

Supplementary Figure 4

Supplementa

ry Figure 4. Ingenuity pathway analysis for RNA seq differentially expressed genes. All significant pathways are shown, colored by activation direction. Orange denotes pathway activation in PDCL compared to parental tumors and blue denoted pathway inhibition, grey denotes that activation direction could not be inferred.

Supplementary Table 1. Tumor and PDCL GBM subtypes.

	Tumor	**PDCL**
3724	proneural	classical
4724	mesenchymal	proneural
3427	classical	classical
2197	mesenchymal	mesenchymal
2211	classical	classical
3716	proneural	classical
3718	classical	classical
3719	classical	proneural
3722	classical	classical

Supplementary Table 2.OX40 pathway gene list with expression mode

Gene	Affymetrix	Exp Log Ratio	Exp p-value	Expected	Location	Type(s)
B2M	232311_at	-1.236	5.89E-03		Plasma Membrane	transmembrane receptor
CD4	203547_at	-0.478	3.28E-03	Down	Plasma Membrane	transmembrane receptor
FCER1G	204232_at	-4.541	2.96E-10	Up	Plasma Membrane	transmembrane receptor
HLA-A	215313_x_at	-0.896	3.43E-03		Plasma Membrane	other
HLA-B	208729_x_at	-1.591	3.44E-03		Plasma Membrane	transmembrane receptor
HLA-DMA	217478_s_at	-4.12	1.26E-06		Plasma Membrane	transmembrane receptor
HLA-DMB	203932_at	-3.464	1.26E-07		Plasma Membrane	transmembrane receptor
HLA-DOA	226878_at	-2.499	6.84E-06		Plasma Membrane	transmembrane receptor
HLA-DPA1	211990_at	-6.418	1.09E-07		Plasma Membrane	transmembrane receptor
HLA-DPB1	201137_s_at	-5.778	3.07E-07		Plasma Membrane	transmembrane receptor
HLA-DQB1	212998_x_at	-4.279	5.59E-09		Plasma Membrane	other
HLA-DRA	208894_at	-5.909	1.97E-07		Plasma Membrane	transmembrane receptor
HLA-E	200904_at	-3.086	4.62E-06		Plasma Membrane	transmembrane receptor
HLA-F	221875_x_at	-1.501	2.85E-03		Plasma Membrane	transmembrane receptor
HLA-G	211529_x_at	-1.236	5.24E-03		Plasma Membrane	other
MAP2K4	203265_s_at	0.996	1.35E-03	Up	Cytoplasm	kinase
MAPK8	226048_at	0.761	3.79E-04	Up	Cytoplasm	kinase
MAPK9	210570_x_at	1.056	7.95E-04	Up	Cytoplasm	kinase
NFKBIA	201502_s_at	-1.765	1.36E-05	Down	Cytoplasm	transcription regulator
TNFRSF4	214228_x_at	-0.376	3.37E-03	Up	Plasma Membrane	transmembrane receptor

Supplementary Table 3. Upstream regulators for microarray data. Top predicted upstream regulators (p<1E-5). Log expression value is given (in case directly measured in the differentially expressed genes). Activation z - scores of PDCL vs. tumors along with predicted activation (in case |z|>2) are given.

Legend. NA – not available, TSG – tumor suppressor gene, ECM – extracellular matrix, TF – transcription factor

Predicted Activation Stat	Activation z-score	p-value of over
Activated	5.916	3.67E-14
Inhibited	-4.803	9.21E-11
		5.28E-10
Inhibited	-4.550	1.46E-09
		1.56E-09
	1.980	2.67E-09
	1.513	1.23E-08
	-1.727	3.49E-08
Inhibited	-2.475	6.48E-08
	-0.479	1.64E-07
Inhibited	-3.370	6.40E-07
Inhibited	-6.929	2.26E-06
Inhibited	-2.079	3.23E-06
Activated	2.964	3.45E-06
Inhibited	-6.019	7.85E-06
Activated	3.646	8.47E-06

Supplementary Table 4. RABL6 upstream regulator fingerprint in the microarray data. 35 genes of the fingerprint appear in the 2643 differentially expressed genes. Their log expression ratios (PDCL vs. tumors) are given. Interestingly – all of the genes' log expression ratio supports activation of RABL6 gene.

Genes in dataset	Affimetrix ID	Prediction (based on expression direction)	Exp Log Ratio	Findings
VRK1	203856_at	Activated	1.656	Upregulates
UBE2C	202954_at	Activated	1.473	Upregulates
TTK	204822_at	Activated	2.194	Upregulates
TMEM97	212282_at	Activated	1.627	Upregulates
RFC3	204128_s_at	Activated	2.279	Upregulates
RAD54B	219494_at	Activated	1.747	Upregulates
PTPRM	1555579_s_at	Activated	-2.552	Downregulates
PSME3	209853_s_at	Activated	0.99	Upregulates
PRIM1	205053_at	Activated	2.123	Upregulates
PRC1	218009_s_at	Activated	1.21	Upregulates
POLE2	205909_at	Activated	1.903	Upregulates
PBK	219148_at	Activated	2.166	Upregulates
PARP2	215773_x_at	Activated	0.889	Upregulates
NEK2	204641_at	Activated	1.636	Upregulates
NDC80	204162_at	Activated	1.751	Upregulates
MELK	204825_at	Activated	1.562	Upregulates
MCM10	220651_s_at	Activated	2.657	Upregulates
MAD2L1	1554768_a_at	Activated	2.489	Upregulates
KIF23	204709_s_at	Activated	2.599	Upregulates
HMOX1	203665_at	Activated	-2.047	Downregulates
HMMR	209709_s_at	Activated	2.374	Upregulates
FRMD4A	1560031_at	Activated	-1.824	Downregulates
EZH2	203358_s_at	Activated	1.358	Upregulates
DUT	208955_at	Activated	1.452	Upregulates
CKS1B	201897_s_at	Activated	1.786	Upregulates
CHEK2	210416_s_at	Activated	1.55	Upregulates
CHEK1	205394_at	Activated	2.122	Upregulates
CENPF	209172_s_at	Activated	1.875	Upregulates
CDC25C	205167_s_at	Activated	1.848	Upregulates
CDC25A	204695_at	Activated	1.068	Upregulates
CCNB1	214710_s_at	Activated	1.652	Upregulates
CCNA2	203418_at	Activated	1.927	Upregulates
BUB1B	203755_at	Activated	1.375	Upregulates
BUB1	209642_at	Activated	2.228	Upregulates
AURKB	209464_at	Activated	1.581	Upregulates

Supplementary Table 5.GSEA pathways overrepresented in GBM-PDCL (nominal p value <0.05)

Legend. Size – number of genes in the pathway list. ES – enrichment score, NES – normalized enrichment score, NOM p-val – nominal p-value, FDR q-val – FDR significance, FWER p-val - Familywise-error rate p – value. RANK AT MAX representsa quantitative parameter of a pathway distribution in the expression data set.

NAME	SIZE	ES	NES	NOM p-val	FDR q-val	FWER p-val	RANK AT MAX
BIOCARTA_ATRBRCA_PATHWAY	21	0.801758	2.004002	0	0.020601	0.023	922
KEGG_RNA_DEGRADATION	51	0.715051	1.950301	0	0.036524	0.069	3335
PID_AURORA_B_PATHWAY	37	0.786136	1.950274	0.006	0.024349	0.069	2839
PID_ATR_PATHWAY	38	0.778554	1.932374	0.00809717	0.023872	0.082	2015
PID_ATM_PATHWAY	31	0.708683	1.924177	0.00400802	0.022612	0.092	1901
KEGG_PROTEASOME	42	0.703722	1.920131	0	0.019828	0.095	2885
PID_FANCONI_PATHWAY	42	0.733397	1.91682	0.00404858	0.017501	0.099	1974
KEGG_NUCLEOTIDE_EXCISION_REPAIR	44	0.6095	1.89696	0.00769231	0.021349	0.136	4516
KEGG_MISMATCH_REPAIR	22	0.785334	1.884915	0.00793651	0.022008	0.15	2096
KEGG_SPLICEOSOME	96	0.617386	1.883901	0.00398406	0.020165	0.153	3135
KEGG_AMINOACYL_TRNA_BIOSYNTHESIS	32	0.737526	1.824829	0.00398406	0.038198	0.243	3728
PID_DNA_PK_PATHWAY	15	0.71025	1.818089	0.00193424	0.038691	0.261	3419
PID_P53_REGULATION_PATHWAY	55	0.583678	1.803001	0.00790514	0.042081	0.292	4536
PID_PLK1_PATHWAY	39	0.680266	1.782139	0.02862986	0.049703	0.344	2915
KEGG_PYRUVATE_METABOLISM	40	0.565402	1.780812	0.00793651	0.047023	0.348	1898
KEGG_TERPENOID_BACKBONE_BIOSYNTHESIS	15	0.786456	1.777739	0.00776699	0.04589	0.356	2972
KEGG_CELL_CYCLE	113	0.573766	1.764343	0.03846154	0.050386	0.388	3478
KEGG_CITRATE_CYCLE_TCA_CYCLE	29	0.703399	1.762925	0.00811359	0.048216	0.392	3332
BIOCARTA_PROTEASOME_PATHWAY	26	0.76484	1.76265	0.00196464	0.045789	0.393	2885
BIOCARTA_G2_PATHWAY	23	0.676678	1.757722	0.01364522	0.045599	0.406	3922
KEGG_DNA_REPLICATION	34	0.73251	1.745932	0.04347826	0.049161	0.434	2103
KEGG_HUNTINGTONS_DISEASE	164	0.539402	1.739296	0.01782178	0.050079	0.453	4226
PID_FOXM1_PATHWAY	39	0.657554	1.731489	0.0417495	0.051747	0.474	3994
PID_BARD1_PATHWAY	29	0.701185	1.73024	0.0260521	0.050347	0.477	1867
KEGG_BASAL_TRANSCRIPTION_FACTORS	33	0.604937	1.726874	0.0040568	0.05005	0.487	4384
PID_TELOMERASE_PATHWAY	65	0.474336	1.726587	0.00814664	0.048268	0.488	5009
KEGG_PYRIMIDINE_METABOLISM	88	0.550056	1.715579	0.01568628	0.052106	0.523	4870
PID_MYC_ACTIV_PATHWAY	75	0.526583	1.713285	0.02195609	0.051285	0.526	5908
KEGG_PARKINSONS_DISEASE	106	0.592141	1.705147	0.02755906	0.053104	0.543	3332
KEGG_STEROID_BIOSYNTHESIS	16	0.771256	1.70384	0.01160542	0.051918	0.547	3837
KEGG_OOCYTE_MEIOSIS	106	0.448613	1.69676	0.02653061	0.05387	0.572	5171
KEGG_UBIQUITIN_MEDIATED_PROTEOLYSIS	122	0.470722	1.695734	0.01008065	0.05277	0.575	5996
BIOCARTA_MEF2D_PATHWAY	18	0.533271	1.691715	0.00393701	0.053068	0.587	1962
KEGG_OXIDATIVE_PHOSPHORYLATION	110	0.588564	1.676911	0.04863813	0.058762	0.636	5614
KEGG_ALZHEIMERS_DISEASE	149	0.492881	1.656699	0.03937008	0.069076	0.691	3332
BIOCARTA_ATM_PATHWAY	20	0.550716	1.646235	0.02264151	0.072899	0.721	2155
KEGG_BASE_EXCISION_REPAIR	33	0.582175	1.640244	0.04142012	0.074216	0.729	5149
KEGG_CYSTEINE_AND_METHIONINE_METABOLISM	31	0.52323	1.630944	0.01785714	0.078097	0.759	3373
PID_E2F_PATHWAY	65	0.533747	1.622836	0.04907975	0.081488	0.778	3922
KEGG_HOMOLOGOUS_RECOMBINATION	26	0.628264	1.621542	0.0242915	0.080384	0.781	2481
KEGG_PROPANOATE_METABOLISM	31	0.560408	1.613702	0.04462475	0.084236	0.794	4395
PID_AURORA_A_PATHWAY	29	0.582553	1.59927	0.03822938	0.092157	0.821	2839
KEGG_RNA_POLYMERASE	28	0.628275	1.541259	0.046	0.137493	0.898	2380
PID_MYC_PATHWAY	23	0.589525	1.536046	0.03877551	0.139278	0.904	3378
PID_LIS1_PATHWAY	27	0.463819	1.471095	0.04715128	0.19578	0.955	3923
PID_HIF1A_PATHWAY	18	0.484057	1.463401	0.03393214	0.196878	0.958	1308
PID_LKB1_PATHWAY	37	0.395196	1.423087	0.02366864	0.220762	0.973	4779
KEGG_BIOSYNTHESIS_OF_UNSATURATED_FATTY_ACIDS	19	0.421997	1.410822	0.04150198	0.232981	0.977	4395
PID_AR_TF_PATHWAY	47	0.339221	1.369876	0.03245436	0.269474	0.99	4465

Supplementary Table 6. GSEA pathways overrepresented in tumors.(nominal p value <0.05)

Legend. Size – number of genes in the pathway list. ES – enrichment score, NES – normalized enrichment score, NOM p-val – nominal p-value, FDR q-val – FDR significance, FWER p-val - Familywise-error rate p – value. RANK AT MAX representsa quantitative parameter of a pathway distribution in the expression data set.

NAME	SIZE	ES	NES	NOM p-val	FDR q-val	FWER p-val	RANK AT MAX
KEGG_FC_GAMMA_R_MEDIATED_PHAGOCYTOSIS	87	-0.58529	-2.01951	0	0.01409	0.012	1602
PID_PI3KCI_PATHWAY	41	-0.60021	-1.99169	0.00404858	0.012302	0.02	1134
KEGG_CELL_ADHESION_MOLECULES_CAMS	125	-0.60985	-1.99008	0	0.008987	0.021	3312
KEGG_LEUKOCYTE_TRANSENDOTHELIAL_MIGRATION	107	-0.52996	-1.9715	0	0.0092	0.028	2079
KEGG_VIRAL_MYOCARDITIS	67	-0.61757	-1.90766	0.00205761	0.025306	0.076	2257
KEGG_NATURAL_KILLER_CELL_MEDIATED_CYTOTOXICITY	129	-0.4867	-1.90312	0	0.022987	0.08	2130
KEGG_TYPE_I_DIABETES_MELLITUS	40	-0.69598	-1.87268	0.0020202	0.034934	0.132	2055
KEGG_COMPLEMENT_AND_COAGULATION_CASCADES	66	-0.5952	-1.8669	0.01041667	0.034502	0.144	2267
KEGG_LEISHMANIA_INFECTION	62	-0.70835	-1.85429	0.0020284	0.03851	0.171	2016
KEGG_HEMATOPOIETIC_CELL_LINEAGE	83	-0.6122	-1.85186	0.01232033	0.035707	0.175	2976
KEGG_B_CELL_RECEPTOR_SIGNALING_PATHWAY	71	-0.50058	-1.80959	0.00200803	0.060671	0.269	1929
KEGG_INTESTINAL_IMMUNE_NETWORK_FOR_IGA_PRODUCTION	45	-0.6768	-1.7975	0.00596422	0.065848	0.292	3765
KEGG_ASTHMA	27	-0.74709	-1.79607	0.01010101	0.061688	0.293	2018
PID_INTEGRIN2_PATHWAY	28	-0.66951	-1.79589	0.02070393	0.0576	0.293	3707
KEGG_AUTOIMMUNE_THYROID_DISEASE	49	-0.67302	-1.79477	0.00806452	0.054084	0.293	2055
BIOCARTA_SPPA_PATHWAY	19	-0.57569	-1.78769	0.00199203	0.056684	0.314	1005
PID_TXA2PATHWAY	55	-0.52219	-1.783	0.00604839	0.056643	0.326	3871
BIOCARTA_RHO_PATHWAY	31	-0.61075	-1.77623	0.00416667	0.057698	0.345	1937
BIOCARTA_DC_PATHWAY	22	-0.62487	-1.77578	0.01012146	0.054775	0.345	2018
KEGG_GRAFT_VERSUS_HOST_DISEASE	37	-0.74679	-1.77049	0.00416667	0.056307	0.363	2055
KEGG_ALLOGRAFT_REJECTION	34	-0.75684	-1.77018	0	0.053757	0.364	2055
KEGG_REGULATION_OF_ACTIN_CYTOSKELETON	196	-0.41145	-1.76507	0	0.054141	0.378	1603
PID_CXCR4_PATHWAY	97	-0.49806	-1.75548	0.00835073	0.05772	0.414	2532
BIOCARTA_COMP_PATHWAY	16	-0.7242	-1.74262	0.03238867	0.064211	0.45	2019
PID_HIF1_TFPATHWAY	60	-0.528	-1.73442	0.01207244	0.067644	0.47	2470
PID_INTEGRIN_A4B1_PATHWAY	33	-0.54381	-1.72759	0.00838574	0.070361	0.491	2584
PID_IL8_CXCR2_PATHWAY	30	-0.59367	-1.7268	0.01397206	0.068265	0.491	1288
PID_INTEGRIN1_PATHWAY	64	-0.60158	-1.7246	0.02910603	0.067243	0.494	4235
PID_INTEGRIN3_PATHWAY	42	-0.6656	-1.71845	0.03036437	0.069798	0.511	4232
PID_FCER1_PATHWAY	58	-0.50159	-1.71501	0.00603622	0.070114	0.522	1784
KEGG_ECM_RECEPTOR_INTERACTION	81	-0.56022	-1.7102	0.03389831	0.07144	0.534	4372
PID_AMB2_NEUTROPHILS_PATHWAY	41	-0.56027	-1.69466	0.02653061	0.080925	0.574	1879
BIOCARTA_NKT_PATHWAY	27	-0.59076	-1.6909	0.02208835	0.081625	0.589	2426
BIOCARTA_IL22BP_PATHWAY	16	-0.72381	-1.68092	0.0239521	0.088168	0.617	3363
PID_RAC1_REG_PATHWAY	36	-0.49933	-1.67857	0.01622718	0.08776	0.624	2875
PID_AVB3_INTEGRIN_PATHWAY	72	-0.50507	-1.67546	0.02474227	0.088658	0.636	4353
PID_ALK1_PATHWAY	26	-0.53766	-1.67539	0.01992032	0.086318	0.636	2776
PID_IL8_CXCR1_PATHWAY	25	-0.60172	-1.66831	0.01606426	0.090058	0.653	1134
PID_INTEGRIN_A9B1_PATHWAY	23	-0.6437	-1.66498	0.0042735	0.090513	0.666	2013
PID_INTEGRIN5_PATHWAY	17	-0.68443	-1.65277	0.01882845	0.099534	0.698	4655
BIOCARTA_PPARA_PATHWAY	53	-0.42944	-1.64417	0.00769231	0.103038	0.721	3746
BIOCARTA_MYOSIN_PATHWAY	30	-0.51068	-1.63864	0.02484472	0.105656	0.732	5233
BIOCARTA_FCER1_PATHWAY	37	-0.48315	-1.63047	0.0134357	0.110717	0.748	1784
KEGG_FC_EPSILON_RI_SIGNALING_PATHWAY	75	-0.40028	-1.62385	0.01953125	0.114287	0.755	1134
BIOCARTA_IL7_PATHWAY	17	-0.63387	-1.62262	0.02772277	0.11309	0.757	3361
PID_GMCSF_PATHWAY	37	-0.50421	-1.60264	0.04098361	0.130152	0.794	1334
KEGG_DILATED_CARDIOMYOPATHY	89	-0.45294	-1.59512	0.03298969	0.134982	0.806	4796
PID_TCPTP_PATHWAY	40	-0.47548	-1.59421	0.03305785	0.133068	0.807	3528
PID_NFKAPPAB_ATYPICAL_PATHWAY	17	-0.55252	-1.5881	0.02016129	0.137511	0.82	1534
KEGG_TYPE_II_DIABETES_MELLITUS	44	-0.44373	-1.58794	0.0234375	0.134969	0.82	4792
KEGG_CHEMOKINE_SIGNALING_PATHWAY	173	-0.39965	-1.58734	0.02240326	0.132947	0.823	4032
KEGG_PHOSPHATIDYLINOSITOL_SIGNALING_SYSTEM	67	-0.42496	-1.58729	0.00420168	0.130511	0.823	1321
PID_TOLL_ENDOGENOUS_PATHWAY	23	-0.59313	-1.58387	0.01006036	0.129844	0.826	361
KEGG_FOCAL_ADHESION	188	-0.42546	-1.58016	0.04968944	0.131038	0.836	3262
PID_ENDOTHELIN_PATHWAY	62	-0.45686	-1.57529	0.02	0.13191	0.851	1800
BIOCARTA_CSK_PATHWAY	23	-0.51564	-1.57246	0.04101563	0.132705	0.858	3696
KEGG_VASCULAR_SMOOTH_MUSCLE_CONTRACTION	110	-0.42209	-1.56495	0.0376569	0.135975	0.872	4401
KEGG_ALDOSTERONE_REGULATED_SODIUM_REABSORPTION	40	-0.40937	-1.55684	0.02028398	0.14269	0.889	2104
PID_AP1_PATHWAY	69	-0.41922	-1.542	0.02788845	0.152064	0.904	3966
BIOCARTA_TID_PATHWAY	19	-0.5781	-1.53421	0.04276986	0.158143	0.913	4541
PID_BCR_5PATHWAY	64	-0.43152	-1.52758	0.0334728	0.162667	0.922	1602
KEGG_PRION_DISEASES	35	-0.41696	-1.50868	0.03131524	0.171393	0.933	4015
PID_ALPHA_SYNUCLEIN_PATHWAY	33	-0.50272	-1.50058	0.04868154	0.173707	0.94	1210
KEGG_ARRHYTHMOGENIC_RIGHT_VENTRICULAR_CARDIOMYOPATHY_ARVC	73	-0.42256	-1.48775	0.03278688	0.177057	0.944	5677
PID_GLYPICAN_1PATHWAY	25	-0.52909	-1.48164	0.03118503	0.177826	0.945	1705
KEGG_TRYPTOPHAN_METABOLISM	38	-0.41572	-1.46798	0.04117647	0.187059	0.951	2714
BIOCARTA_ALK_PATHWAY	36	-0.42067	-1.45204	0.03838772	0.197374	0.956	2234
KEGG_INOSITOL_PHOSPHATE_METABOLISM	46	-0.39662	-1.44743	0.03092784	0.200628	0.959	1134
KEGG_TGF_BETA_SIGNALING_PATHWAY	82	-0.34103	-1.41861	0.03193613	0.215834	0.968	2475
KEGG_CALCIUM_SIGNALING_PATHWAY	171	-0.3327	-1.41196	0.04285714	0.220134	0.971	4087
KEGG_ADHERENS_JUNCTION	73	-0.34589	-1.41173	0.03665988	0.216287	0.971	2700
KEGG_PPAR_SIGNALING_PATHWAY	66	-0.35888	-1.40718	0.04216867	0.215922	0.973	2574
KEGG_PANCREATIC_CANCER	69	-0.32231	-1.29832	0.036	0.303675	0.991	2425

Supplementary Table 7. Top predicted upstream regulators for RNA-seq data (p<1E-5). Log expression value is given (in case directly measured in the differentially expressed genes). Activation z - scores of PDCL vs. tumors along with predicted activation (in case |z|>2) are given.

Upstream Regulator	Exp Log	Molecule Type	Predicted Activatio	Activation z-scor	p-value of overlap
E2F4	-0.064	transcription regulator			1.37E-16
MITF	-0.593	transcription regulator	Activated	6.142	3.31E-11
RABL6	0.138	other	Activated	6.252	8.19E-11
TGM2	-3.58	enzyme	Inhibited	-7.621	2.68E-09
IL13	-2.043	cytokine		0.114	3.07E-08
E2F1	1.21	transcription regulator		-0.168	3.16E-08
TP53	0.174	transcription regulator	Inhibited	-5.806	1.36E-07
SPI1	-8.88	transcription regulator		0.304	1.72E-07
NUPR1	-2.118	transcription regulator	Inhibited	-10.012	2.44E-07
CD40LG	-5.582	cytokine	Inhibited	-3.933	7.03E-07
CEBPA	-2.759	transcription regulator	Inhibited	-3.196	1.11E-06
CCND1	0.617	transcription regulator	Activated	2.209	1.43E-06
IFNG	-0.513	cytokine	Inhibited	-6.224	3.73E-06
FOXM1	1.803	transcription regulator	Activated	3.903	3.93E-06
IL27	-5.656	cytokine	Inhibited	-2.189	4.56E-06
CDK4	0.783	kinase			6.18E-06
FOXO1	-0.732	transcription regulator		0.102	6.51E-06
CD3		complex	Activated	3.252	6.77E-06
HCAR2	-5.025	g-protein coupled receptor		-1.508	7.41E-06
IL1B	-5.467	cytokine	Inhibited	-4.952	8.10E-06